



Published in final edited form as:

*J Orthop Res.* 2012 May ; 30(5): 693–699. doi:10.1002/jor.22001.

## Viscoelastic properties of human cortical bone tissue depend on gender and elastic modulus

Ziheng Wu, Timothy C. Ovaert, and Glen L. Niebur

Tissue Mechanics Laboratory, Department of Aerospace and Mechanical Engineering, University of Notre Dame, Notre Dame, IN 46556, USA

### Abstract

Bone exhibits rate dependent failure behavior, suggesting that viscoelasticity is a factor in the damage and fracture of bone. Microdamage initiates at scales below the macroscopic porosity in bone, and, as such, is affected by the intrinsic viscoelasticity of the bone tissue. The viscoelasticity of the bone tissue can be measured by nanoindentation and recording the creep behavior at constant load. The viscoelastic properties have been used to assess differences in tissue behavior with respect to fracture healing, aging, and mouse strains. In this study we compared the viscoelastic behavior of human cortical bone between genders by using nanoindentation at a fixed load of 10 mN to measure the creep time constant. Bones from females had a significantly greater time constant, indicating slower creep and relaxation, than bones from males. The creep time constants decreased with increasing tissue modulus. The mineralization, collagen content, and collagen cross-link density, which were bulk measurements, were analyzed to determine if the differences in viscoelastic behavior were explained by compositional differences in the bone. However, none of the parameters differed between genders, nor were they correlated to the viscoelastic time constant. As such, the difference must depend on other matrix proteins that we did not assess or differences in the microstructural organization. This is one of the only intrinsic bone material properties that has been found to differ between males and females, and it may be important for assessing differences in fracture risk, since crack propagation is generally sensitive to viscoelastic properties.

### Keywords

Bone quality; Gender; Nanoindentation; Mineralization; Collagen

### Introduction

Bone is a viscoelastic material, that exhibits both creep and stress relaxation.<sup>1</sup> The ultimate strength,<sup>2</sup> energy to failure<sup>3</sup> and fracture toughness<sup>4</sup> of bone tissue are rate dependent. The fatigue life of bone is also frequency dependent,<sup>5</sup> and crack growth is both cycle and frequency dependent at high stress intensity.<sup>6</sup> As such, the viscoelastic properties of bone may play a role in fracture.<sup>7</sup> However, bone is a hierarchical composite, and the viscoelastic properties may differ between microstructural and macroscopic levels.

---

Address Correspondence and Reprint Requests to: Glen L. Niebur, Ph. D., Associate Professor, Department of Aerospace and Mechanical Engineering, University of Notre Dame, Notre Dame, IN 46556, Phone: (574) 631 3327, Fax: (574) 631 8341, gniebur@nd.edu.

#### Conflict of Interest:

The authors have no conflicts of interest.

Porosity plays a major role in the macroscopic strength and viscoelasticity of bone. The relaxation time constant is positively correlated to water content in torsion,<sup>8</sup> and hydrated bone exhibits greater viscoelastic damping than dry bone over a broad range of frequencies.<sup>9</sup> At low frequencies, viscoelasticity was attributed to viscous-like motion at the cement lines.<sup>10</sup>

Microdamage occurs at scales below the macroscopic porosity. As such, the intrinsic viscoelasticity at length scales on the order of size of a microcrack may be important. Measurements of the viscoelasticity of bone at the microstructural level have become more common with the availability of nanoindentation.<sup>11–13</sup> The modulus measured by nanoindentation is positively correlated with strain rate and holding time in human cortical bone.<sup>14</sup> In healing porcine bone<sup>15</sup> and canine cortical bone,<sup>16</sup> the viscosity in viscoelastic-plastic<sup>15</sup> and Voigt<sup>16</sup> viscoelastic models increased with modulus, consistent with the dependence on mineralization and modulus at the macroscopic level.<sup>17–18</sup> Viscoelasticity depends on the tissue composition, with both compliance coefficients and time constants associated with water content in spherical indentation creep.<sup>19</sup> Collagen content and chemistry may also play a role in determining viscoelasticity.<sup>20</sup> For example, collagen cross-link concentration depends on both age and gender,<sup>21–22</sup> and could affect the viscoelastic behavior by altering the interface between mineral and collagen phases.<sup>10,23</sup>

Microdamage is more common in the femoral cortical bone of females than males, and increases with age.<sup>24</sup> As fatigue crack propagation is sensitive to viscoelastic behavior,<sup>25–26</sup> we hypothesized that the microstructural level viscoelasticity of female cortical bone differs from males. Moreover, we hypothesized that differences in viscoelasticity are due to differences in bone composition. Therefore, the goal of the study was to investigate the dependence of the microstructural viscoelastic properties of human cortical bone on gender, age, and tissue composition. Specifically, we 1) measured the elastic modulus and creep time constant of human cortical bone in both osteons and interstitial tissue; 2) measured tissue composition including mineralization, collagen content, and collagen cross-link content; and 3) investigated the dependence of the viscoelastic properties on age, gender, microstructural location, and tissue composition.

## Materials and methods

Twenty fresh-frozen human femurs, ten male and ten female of similar age range, were obtained from a national donor network under informed consent (National Disease Research Interchange). The donors had no history of liver or kidney disease, hyper- or hypoparathyroidism, alcoholism, bone diseases, recent fractures, or medication for osteoporosis. The mean age of the males was  $70 \pm 12$  (mean  $\pm$  standard deviation), ranging from 51 to 87, and that of the females was  $76 \pm 11$  yrs, ranging from 58 to 89.

Small trapeziform blocks, approximately 5 mm thick, were cut from the posterior mid-diaphysis of each femur using a diamond saw (Buehler, Lake Bluff, IL). One cross-sectional surface of the sample was fixed to a metal disk with cyanoacrylate glue, while the opposite side was polished with successive grades of abrasives starting with 800 grit paper and ending with 0.25  $\mu\text{m}$  alumina suspension. The bone was kept hydrated with deionized water throughout cutting and polishing. Samples were stored at  $-20^\circ\text{C}$  in buffered saline saturated gauze until nanoindentation, then thawed and stored in buffered saline until immediately prior to testing.

The samples were subjected to nanoindentation to measure elastic and viscoelastic properties. Forty indents, 20 in different osteon and 20 in the adjacent interstitial tissue spread across the surface of the bone (Fig. 1) were made using a nanoindenter (Hysitron,

Minneapolis, MN) fitted with a Berkovich pyramidal tip. The tip function of the system is regularly calibrated on a fused quartz sample. The indenter was advanced at a rate of 2.0 mN/s to 10 mN, held at constant load for 10 seconds, and unloaded at 2.0 mN/s.

The viscoelastic properties were found by fitting the indentation depth-time curve to a Burgers model (Fig. 2a) given by:

$$h^2(t) = \frac{\pi}{2} P_0 \cot \alpha \left[ \frac{1}{E_1} + \frac{1}{E_2} (1 - e^{-t/\tau}) + \frac{1}{\eta_1} t \right] \quad (1)$$

where  $h(t)$  is the indentation depth,  $P_0$  is the peak force,  $\alpha$  is the equivalent cone semi-angle, ( $70.3^\circ$  for a Berkovich indenter),  $E_1$  is the instantaneous modulus (GPa) while  $(E_1 E_2) / (E_1 + E_2)$  is the relaxed modulus,  $\tau$  is the creep time constant (s), and  $\eta_1$  is a long term creep viscosity (GPa·s).<sup>27</sup> The creep time constant is associated with an exponential decay to a steady state deformation, with a larger time constant indicating slower creep under static loading. The reciprocal of the long term viscosity,  $\eta_1$ , is associated with a continuous deformation rate under constant load. In real solids, this behavior does not exist. However for finite holding time, it provides a means to characterize a secondary, slow, creep process. The measured creep time constant and long-term viscosity did not exhibit a trend during the approximately 30 minutes required for testing, indicating that the results were not affected by specimen drying during the test period. All of the mechanical parameters for each model were determined for each indent, and averaged within samples. Although equation (1) ignores the rise, or loading, portion of the curve, the effect of the creep time constant during the holding period is independent of the rise time.<sup>28</sup> Since the loading portion of the curve involves permanent deformation, equation (1) cannot be used to determine the moduli,<sup>13</sup> as elastic and permanent portions of the deformation cannot be separated. As such, the indentation modulus was measured from the unloading curve.<sup>29</sup>

The tissue level mineral density (TMD) of the samples was measured by micro-CT (Scanco  $\mu$ CT-80, Brüttisellen, Switzerland). The samples were scanned at 10  $\mu$ m resolution while immersed in buffered saline. The X-ray energy spectrum was 70 kVp, at 114  $\mu$ A. The integration time was 210 ms. Beam hardening and anti-ring corrections were applied during reconstruction. A Gaussian filter with support 1 and sigma 0.9 was applied to the reconstructed images. The filtered images were thresholded (lower threshold 553 mg HA/cm<sup>3</sup>) and the mean TMD was found using a custom non-linear calibration equation based on an HA-polyethylene phantom.<sup>30</sup>

The organic and inorganic fractions were also measured by ashing.<sup>31</sup> The hydrated weight was measured, and the volume and apparent density of each sample were measured by Archimedes's principle. The samples were then dried at 90 °C for 24 hours, and the dry weight was measured. Finally, samples were ashed at 600 °C for 24 hours, and the resulting ash weighed. The ash density was calculated as ash weight divided by the original volume, the organic weight as dry weight minus ash weight and organic density as organic weight divided by the original volume.

Concentrations of collagen cross-links were measured by high performance liquid chromatography (HPLC).<sup>32</sup> Briefly, approximately 10 mg of material was cut from the samples measured by nanoindentation. This material was dehydrated by soaking in successive concentrations of ethanol for 2h, and left overnight in pure ethanol. After dehydration, samples were dried for 8 h in an oven at 90°C, and their masses were measured with a precision balance (AG204, Mettler Toledo, Greifensee, Switzerland). The dehydrated samples were hydrolyzed in 500  $\mu$ L of 6 N HCl at 110°C for at least 20 h. The hydrolysate was split into two at a nominal ratio of 65:35 using the larger sample for cross-link

quantification and the smaller for hydroxyproline quantification. For cross-link measurement, the acid was removed in a vacuum oven at 65° C. HPLC (Waters 2695, Milford, MA) was performed, and hydroxylysylpyridinoline (HP), lysylpyridinoline (LP) and pentosidine (PE) cross-links were quantified by comparison to known standards (HP and LP standards from Pyd/Dpd HPLC Calibrator, Quidel Corp., San Diego, CA; PE standard from International Malliard Reaction Society). The hydroxyproline content was similarly measured by HPLC using a hydroxyproline standard (Sigma-Aldrich, St. Louis, MO),<sup>33</sup> and the cross-link concentrations were normalized by the collagen concentration.

The dependence of the creep time constant on age, gender, tissue type, elastic modulus, and tissue composition was determined using generalized linear models (GLM) (JMP, SAS Institute, Cary, NC). Differences in the tissue composition between genders were assessed by Student's t-test.

## Results

The indentation modulus of the interstitial tissue was  $20.15 \pm 3.51$  GPa (Mean  $\pm$  S.D.), while that of the osteonal tissue was  $16.50 \pm 3.46$  GPa ( $p = 0.003$ ). Within a sample, the coefficient of variation of the modulus measurements was  $13.36\% \pm 1.07\%$  for interstitial tissue and  $15.79\% \pm 2.19\%$  for osteonal tissue, on average. The modulus did not depend on age or gender for either tissue type ( $p = 0.7$ , GLM).

The tissue composition was similar between males and females (Table 1). Both ash density and TMD were similar between males and females ( $p > 0.7$ ) and independent of age ( $p > 0.4$ ). Similarly, the cross-link concentrations, organic fraction, and collagen content did not depend on gender or age ( $p > 0.1$ , GLM). In general, the compositional measures were not correlated (Table. 2), except the HP and LP concentrations were strongly correlated to one another ( $r^2 > 0.84$ ,  $p < 0.001$ , ANCOVA). The mean TMD was similar to ash density ( $p = 0.4$ , paired T-test), but they were not correlated, which may be due to the small range of values.

The modulus depended on bulk mineralization but the results were sensitive to the measurement method. The modulus of the osteonal tissue increased with TMD ( $p = 0.02$ ,  $R^2 = 0.24$ ), and the dependence on ash density was marginally significant ( $p = 0.052$ ). In contrast, the modulus of the interstitial tissue increased with ash density ( $p = 0.03$ ,  $R^2 = 0.25$ ), but was marginally correlated to TMD ( $p = 0.07$ , linear regression).

The Burgers model captured the time dependent creep behavior. The squared correlation coefficient ( $R^2$ ) was 0.99 for all indents (Fig. 2b). Within samples, the coefficient of variation of the creep time constant averaged  $18.3\% \pm 3.87\%$  for interstitial tissue and  $17.7\% \pm 4.13\%$  for osteonal tissue, on average.

The creep time constant decreased with increasing modulus ( $p < 0.003$ , GLM; Fig. 3). The slope of the regressions was independent of gender ( $p > 0.06$ ), but the intercepts differed ( $p < 0.005$ ), and the adjusted mean creep time constant was nearly 15% higher for females than males ( $p < 0.005$ ). On average, the creep time constant was higher in osteonal bone than in interstitial bone (two-factor ANOVA), but after accounting for the effect of modulus by GLM, there was no difference in creep time constant between the two tissue types. Similarly, the creep constant did not depend on TMD ( $p = 0.18$ ), ash density ( $p = 0.22$ ), organic fraction ( $p = 0.90$ ), collagen content ( $p = 0.47$ ), nor collagen cross-link density ( $p = 0.10$ ) when modulus was included as a covariate. When analyzed separately, the creep time constant was negatively correlated with ash density in the interstitial bone ( $p < 0.03$ ,  $R^2 = 0.35$ , linear regression), but not in osteons ( $p = 0.065$ , Table. 2). When the data sets from the osteonal and interstitial bone were analyzed together, the time constant

decreased with ash density ( $p < 0.01$ ,  $R^2=0.32$ ). This discrepancy may reflect that mineralization was measured for the whole samples rather than separately in the osteons and interstitial tissue that was indented.<sup>21,34-35</sup>

The long-term viscosity,  $\eta_1$ , did not depend on age, TMD, collagen cross-link concentration or elastic modulus ( $p > 0.2$ , linear regression), and was similar between genders and tissue type (ANOVA).

## Discussion

The rate dependence of strength<sup>2</sup> and fatigue strength dependence on frequency<sup>5</sup> suggest that bone viscoelasticity affects fracture behavior. In viscoelastic materials, the viscoelastic time constant affects both the susceptibility to strain controlled fatigue crack growth<sup>36</sup> and the crack growth rate.<sup>25-26</sup> Using nanoindentation, we found that bone from females had a greater creep time constant than males after compensating for differences in age and modulus. This finding indicates that viscoelasticity might play a role in determining fracture risk. The bone mineralization, organic fraction, collagen content, and collagen cross-linking were measured in an effort to identify compositional differences that might explain the differences in material properties. The collagen to mineral or organic fraction to mineral ratios were expected to explain these differences, as ceramics are not viscoelastic at ambient temperature, and creep behavior is generally attributed to the collagen phase of bone.<sup>37</sup> Similarly, differences in collagen cross-link density between genders have been reported,<sup>22</sup> and this was considered as a possible factor explaining differences in viscoelastic behavior. However, none of these factors explained the differences in the properties between genders in these two groups of ten samples.

Some important strengths of this study are that measurements were made in bone from individuals over a wide age range, and in both osteons and interstitial bone. In addition, the composition of the bone (mineral and organic content, and collagen chemistry) was analyzed to identify their relations with viscoelasticity of bone tissue.

The limitations to this study must also be considered. First, we did not separate interstitial tissue from osteons, or measure the tissue composition directly at the site of indentation.<sup>21,34,35</sup> This may have limited our ability to determine the effect of tissue type on mineralization, collagen content, or cross-link density. In a previous study that carefully dissected multiple osteonal and interstitial tissue samples from each bone, the cross-link density differed between male and female bone and depended on age.<sup>22</sup> Second, we did not measure some key compositional quantities, such as mineral crystallinity or calcium to phosphate ratio. These could affect the viscoelastic properties by altering the interfacial binding between the organic and mineral phases.<sup>23</sup> Third, samples were not maintained in a fluid bath during indentation, which might have allowed surface drying in the few microns of depth of the indentations.<sup>16,38</sup> However, the absence of a systematic effect of indentation order on the properties indicates that drying did not affect the creep time constant measurements. Finally, the holding time for creep was short, and the fitted time constants may depend on holding time. However, the relative difference in the time constant between samples increases with holding time,<sup>13</sup> such that the significant differences found here would be found with longer holding times as well.

The microscale measures are an order of magnitude different from the macroscopic values, and the relationship, if any, between the two scales is not known. Macroscopic viscoelasticity involves fluid motion through the pore space as well as interfaces between microstructural components, which may not be captured during nanoindentation.<sup>1,9-10</sup>

Indentation has identified differences in viscoelastic properties in previous studies of bone. In spherical indentation creep of equine bone, the creep time constants in a two-dashpot Kelvin model were both about 1.5 times higher than the present results when fit to the same viscoelastic model (Fig. 4).<sup>19</sup> However, the holding period in<sup>19</sup> was over 10 times longer than used here, and the measured time constants increase with holding time.<sup>13</sup> In addition, spherical indentation results in primarily elastic deformation of the substrate, and allows both the loading and holding portion of the curve to be analyzed. For bovine tibial trabecular and cortical bone indented with a Berkovich indenter, the creep time constant based on Burgers model was on the order of 1 to 5 s,<sup>39</sup> and in a healing rabbit model the time constant ranged from 4 to 5 s,<sup>34</sup> both consistent with the present results. The measured moduli are also consistent with previous nanoindentation and macroscopic studies,<sup>40</sup> as is the weak correlation of modulus to mineralization.<sup>35</sup> However, given the heterogeneity of bone tissue, the correlations in the present study were also limited by the measurement of mineralization at the whole sample level rather than at each indentation location.

The viscoelastic time constant was independent of organic and mineral fractions of the bone, and there was no dependence on collagen cross-linking. Since bone remodeling replaces old tissue with new tissue that is less mineralized, the stable cross-links in the old tissue would be replaced by reducible cross-links in the newly formed tissue. As such, a lower concentration of mature cross-links is expected in osteons than in interstitial bone.<sup>22</sup> If mature cross-links affect the viscoelasticity of bone tissue, a difference between the viscoelasticity of osteons and interstitial bone tissue would have been observed. While the creep time constant was significantly different between the tissue types, this difference was explained by changes in modulus. This agrees with previous reports of differences in the viscosity of younger and older osteons in dogs,<sup>16</sup> which was similarly explained by differences in modulus. Alternate methods, such as Raman spectroscopy<sup>21</sup> and Fourier transform infrared (FTIR) microspectroscopy<sup>34</sup> detected that both modulus and dynamic loss constants were correlated with tissue composition. However, the creep time constant did not depend on any of the compositional measures obtained from FTIR imaging,<sup>34</sup> in agreement with the present results.

Only a few gender differences in bone mechanical properties have been reported. Rat tibiae subjected to fatigue exhibited faster creep rates in females than in males.<sup>41</sup> This is in contrast to the present results where females had higher creep time constants, indicating slower creep. Other differences have been primarily due to differences in bone geometry or size.<sup>42</sup> Overall the composition of bone has been found to be similar between genders in humans<sup>43</sup> and in animals,<sup>44</sup> which complements the findings here. Nyman et al.<sup>22</sup> found gender differences in the concentration of collagen cross-links, which led us to consider this as a source of differences in the time constant. In contrast we found no significant gender differences in cross-linking, although the mean values we measured are similar to previous report.<sup>22</sup> However, Nyman and colleagues measured the collagen cross-link concentration separately in osteonal and interstitial bone tissue, while whole bone samples were processed here. As such, compositional differences may be subtle, and only present in specific microstructural units.

The dependence of viscoelastic properties of bone tissue on gender may play a role in crack propagation and fracture, especially in fatigue loading. Identifying the source of the gender differences may provide insight into new treatment or diagnostic methods, but the compositional measures we considered did not explain them. Other variables that should be considered are mineral crystallinity,<sup>45</sup> the presence of noncollagenous proteins<sup>46-47</sup> that could affect the mineral to organic interface, proteoglycans such as decorin which modulates collagen assembly,<sup>48</sup> and the relative collagen fibril orientations.<sup>49</sup>

## Acknowledgments

This study was supported by the U.S. National Institutes of Health: AR052008. Tissue was obtained from, and screened by, the National Disease Research Interchange. The authors thank Tyler A. Baker for assistance with nanoindentation.

## References

1. Lakes RS, Katz JL, Sternstein SS. Viscoelastic properties of wet cortical bone--I. Torsional and biaxial studies. *Journal of Biomechanics*. 1979; 12:657–678. [PubMed: 489634]
2. Carter DR, Hayes WC. The compressive behavior of bone as a two-phase porous structure. *Journal of Bone and Joint Surgery*. 1977; 59-A:954–962. [PubMed: 561786]
3. Currey JD. Strain rate dependence of the mechanical properties of reindeer antler and the cumulative damage model of bone fracture. *Journal of Biomechanics*. 1989; 22:469–475. [PubMed: 2777821]
4. Kulin RM, Jiang F, Vecchio KS. Effects of age and loading rate on equine cortical bone failure. *J Mech Behav Biomed Mater*. 2011; 4:57–75. [PubMed: 21094480]
5. Wright TM, Hayes WC. The fracture mechanics of fatigue crack propagation in compact bone. *Journal of Biomedical Materials Research*. 1976; 10:637–648. [PubMed: 947925]
6. Nalla RK, Kruzic JJ, Kinney JH, Ritchie RO. Aspects of in vitro fatigue in human cortical bone: time and cycle dependent crack growth. *Biomaterials*. 2005; 26:2183–2195. [PubMed: 15576194]
7. Williams ML. Fracture in viscoelastic media. *Fundamental Phenomena in the Materials Sciences*. 1967; 4:23–32.
8. Sasaki N, Enyo A. Viscoelastic properties of bone as a function of water content. *Journal of Biomechanics*. 1995; 28:809–815. [PubMed: 7657679]
9. Garner E, Lakes R, Lee T, et al. Viscoelastic Dissipation in Compact Bone: Implications for Stress-Induced Fluid Flow in Bone. *Journal of Biomechanical Engineering*. 2000; 122:166–172. [PubMed: 10834157]
10. Lakes RS, Saha S. Cement line motion in bone. *Science*. 1979; 204:501–503. [PubMed: 432653]
11. Rho JY, Roy ME 2nd, Tsui TY, Pharr GM. Elastic properties of microstructural components of human bone tissue as measured by nanoindentation. *J Biomed Mater Res*. 1999; 45:48–54. [PubMed: 10397957]
12. Oyen ML, Cook RF. A practical guide for analysis of nanoindentation data. *J Mech Behav Biomed Mater*. 2009; 2:396–407. [PubMed: 19627846]
13. Wu Z, Baker TA, Ovaert TC, Niebur GL. The effect of holding time on nanoindentation measurements of creep in bone. *J Biomech*. 2011; 44:1066–1072. [PubMed: 21353675]
14. Fan Z, Rho JY. Effects of viscoelasticity and time-dependent plasticity on nanoindentation measurements of human cortical bone. *J Biomed Mater Res A*. 2003; 67:208–214. [PubMed: 14517878]
15. Oyen ML, Ko CC. Examination of local variations in viscous, elastic, and plastic indentation responses in healing bone. *J Mater Sci Mater Med*. 2007; 18:623–628. [PubMed: 17546423]
16. Kim DG, Huja SS, Lee HR, et al. Relationships of viscosity with contact hardness and modulus of bone matrix measured by nanoindentation. *J Biomech Eng*. 2010; 132:024502. [PubMed: 20370248]
17. Les CM, Spence CA, Vance JL, et al. Determinants of ovine compact bone viscoelastic properties: effects of architecture, mineralization, and remodeling. *Bone*. 2004; 35:729–738. [PubMed: 15336610]
18. Sasaki N, Yoshikawa M. Stress relaxation in native and EDTA-treated bone as a function of mineral content. *Journal of Biomechanics*. 1993; 26:77–83. [PubMed: 8423171]
19. Bemby AK, Oyen ML, Bushby AJ, Boyde A. Viscoelastic properties of bone as a function of hydration state determined by nanoindentation. *Philos Mag*. 2006; 86:5691–5703.
20. Donnelly E, Williams RM, Downs SA, et al. Quasistatic and dynamic nanomechanical properties of cancellous bone tissue relate to collagen content and organization. *J Mater Res*. 2006; 21:2106–2117.

21. Donnelly E, Boskey AL, Baker SP, van der Meulen MC. Effects of tissue age on bone tissue material composition and nanomechanical properties in the rat cortex. *J Biomed Mater Res A*. 2010; 92:1048–1056. [PubMed: 19301272]
22. Nyman JS, Roy A, Acuna RL, et al. Age-related effect on the concentration of collagen cross-links in human osteonal and interstitial bone tissue. *Bone*. 2006; 39:1210–1217. [PubMed: 16962838]
23. Lakes RS, Katz JL. Viscoelastic properties of wet cortical bone--II. Relaxation mechanisms. *Journal of Biomechanics*. 1979; 12:679–687. [PubMed: 489635]
24. Norman TL, Wang Z. Microdamage of human cortical bone: incidence and morphology in long bones. *Bone*. 1997; 20:375–379. [PubMed: 9108359]
25. Schapery RA. Theory of Crack Initiation and Growth in Viscoelastic Media .1. Theoretical Development. *Int J Fracture*. 1975; 11:141–159.
26. Schapery RA. Theory of Crack Initiation and Growth in Viscoelastic Media .2. Approximate Methods of Analysis. *Int J Fracture*. 1975; 11:369–388.
27. Fischer-Cripps AC. A simple phenomenological approach to nanoindentation creep. *Materials Science and Engineering A*. 2004; 385:74–82.
28. Oyen ML. Spherical indentation creep following ramp loading. *J Mater Res*. 2005; 20:2094–2100.
29. Oliver. An improved technique for determining hardness and elastic modulus using load and displacement sensing indentation experiments. *J Mater Res*. 1992; 7:1564.
30. Deuerling JM, Rudy DJ, Niebur GL, Roeder RK. Improved accuracy of cortical bone mineralization measured by polychromatic microcomputed tomography using a novel high mineral density composite calibration phantom. *Medical Physics*. 2010; 37:5138–5145. [PubMed: 20964233]
31. Boskey, AL. Bone Mineralization. In: Cowin, SC., editor. *Bone Mechanics Handbook*. 2 ed.. Boca Raton: CRC; 2001. p. 5.1-5.33.
32. Bank RA, Beekman B, Verzijl N, et al. Sensitive fluorimetric quantitation of pyridinium and pentosidine cross-links in biological samples in a single high-performance liquid chromatographic run. *J. Chromatogr. B Biomed. Sci. Appl.* 1997; 703:37–44. [PubMed: 9448060]
33. Bank RA, Jansen EJ, Beekman B, te Koppele JM. Amino acid analysis by reverse-phase high-performance liquid chromatography: improved derivatization and detection conditions with 9-fluorenylmethyl chloroformate. *Anal Biochem*. 1996; 240:167–176. [PubMed: 8811901]
34. Isaksson H, Malkiewicz M, Nowak R, et al. Rabbit cortical bone tissue increases its elastic stiffness but becomes less viscoelastic with age. *Bone*. 2010; 47:1030–1038. [PubMed: 20813215]
35. Zebaze RM, Jones AC, Pandy MG, et al. Differences in the degree of bone tissue mineralization account for little of the differences in tissue elastic properties. *Bone*. 2011; 48:1246–1251. [PubMed: 21385633]
36. Williams, M. Fracture In Viscoelastic Media. In: Bonis, L.; Duga, J.; Gilman, J., editors. *Fundamental Phenomena in the Materials Sciences*. Boston: Plenum Press; 1966. p. 23-32.
37. Bowman SM, Gibson LJ, Hayes WC, McMahon TA. Results from demineralized bone creep tests suggest that collagen is responsible for the creep behavior of bone. *J Biomech Eng*. 1999; 121:253–258. [PubMed: 10211462]
38. Huja SS, Beck FM, Thurman DT. Indentation properties of young and old osteons. *Calcif Tissue Int*. 2006; 78:392–397. [PubMed: 16830198]
39. Isaksson H, Nagao S, Malkiewicz M, et al. Precision of nanoindentation protocols for measurement of viscoelasticity in cortical and trabecular bone. *J Biomech*. 2010; 43:2410–2417. [PubMed: 20478559]
40. Mulder L, Koolstra JH, den Toonder JM, van Eijden TM. Intratrabeular distribution of tissue stiffness and mineralization in developing trabecular bone. *Bone*. 2007; 41:256–265. [PubMed: 17567548]
41. Moreno LD, Waldman SD, Grynblas MD. Sex differences in long bone fatigue using a rat model. *J Orthop Res*. 2006; 24:1926–1932. [PubMed: 16917903]
42. Nieves JW, Formica C, Ruffing J, et al. Males have larger skeletal size and bone mass than females, despite comparable body size. *J Bone Miner Res*. 2005; 20:529–535. [PubMed: 15746999]



43. Pietrzak WS, Woodell-May J, McDonald N. Assay of bone morphogenetic protein-2, -4, and -7 in human demineralized bone matrix. *J Craniofac Surg.* 2006; 17:84–90. [PubMed: 16432413]
44. Bellof G, Most E, Pallauf J. Concentration of Ca, P, Mg, Na and K in muscle, fat and bone tissue of lambs of the breed German Merino Landsheep in the course of the growing period. *J Anim Physiol Anim Nutr (Berl).* 2006; 90:385–393. [PubMed: 16958795]
45. Gourion-Arsiquaud S, Allen MR, Burr DB, et al. Bisphosphonate treatment modifies canine bone mineral and matrix properties and their heterogeneity. *Bone.* 2010; 46:666–672. [PubMed: 19925895]
46. Ingram RT, Park YK, Clarke BL, Fitzpatrick LA. Age- and gender-related changes in the distribution of osteocalcin in the extracellular matrix of normal male and female bone. Possible involvement of osteocalcin in bone remodeling. *J Clin Invest.* 1994; 93:989–997. [PubMed: 8132785]
47. Kavukcuoglu NB, Patterson-Buckendahl P, Mann AB. Effect of osteocalcin deficiency on the nanomechanics and chemistry of mouse bones. *J Mech Behav Biomed Mater.* 2009; 2:348–354. [PubMed: 19627841]
48. Mochida Y, Parisuthiman D, Pornprasertsuk-Damrongsri S, et al. Decorin modulates collagen matrix assembly and mineralization. *Matrix Biol.* 2009; 28:44–52. [PubMed: 19049867]
49. Deuerling JM, Yue W, Espinoza Orias AA, Roeder RK. Specimen-specific multi-scale model for the anisotropic elastic constants of human cortical bone. *J Biomech.* 2009; 42:2061–2067. [PubMed: 19664772]

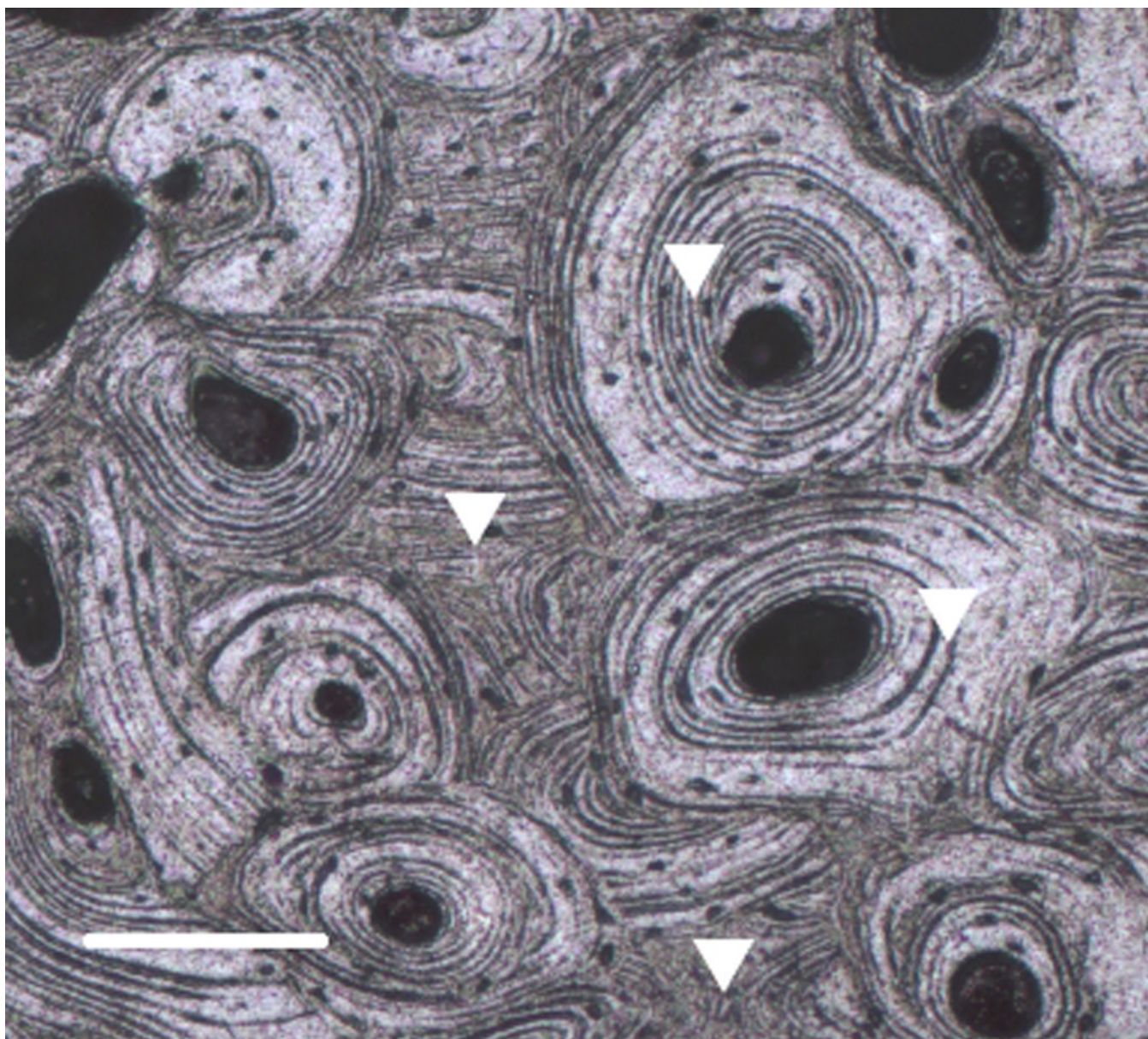


**Figure 1.**  
A micrograph of the polished surface of a cortical bone sample showing typical indentation locations. Bar = 0.5 mm.

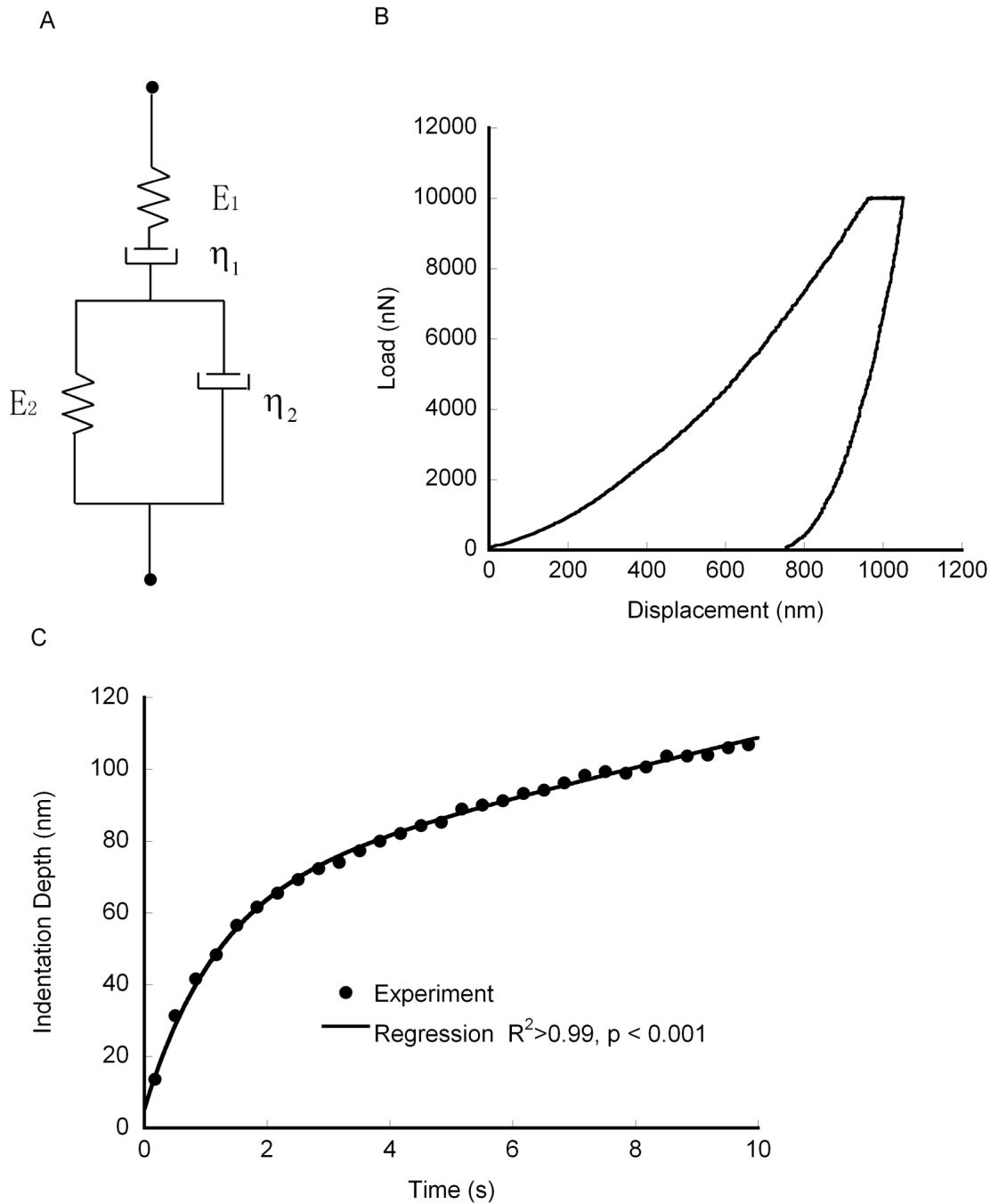


**Figure 2.** a) A spring-dashpot representation of the Burgers viscoelastic element, b) a representative indentation force vs. indentation depth curve, and c) a representative curve fit of the Burgers model to the holding portion of an indentation curve and all curve fits had squared correlation coefficients ( $R^2$ ) over 0.99.

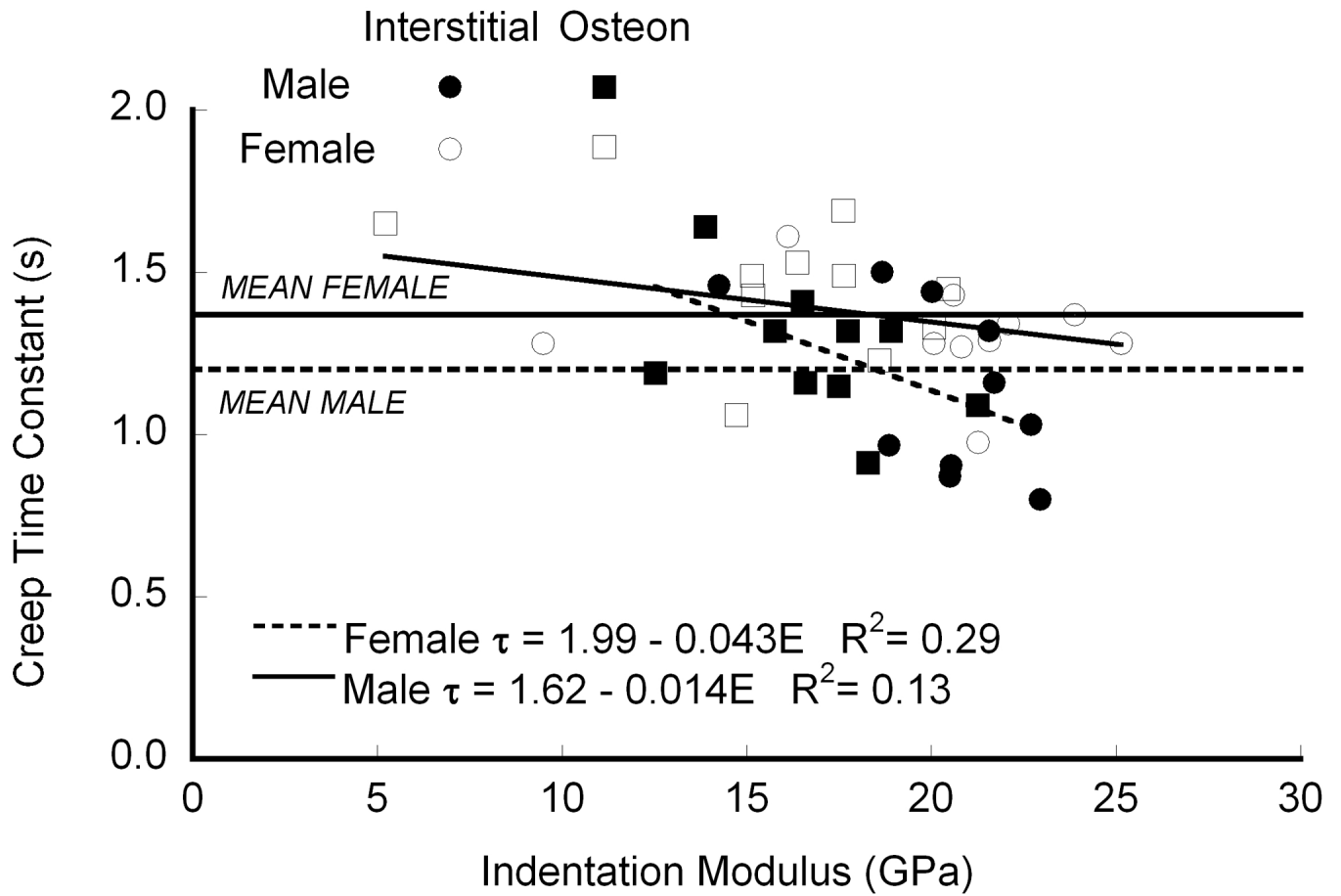


**Figure 3.**

The time constant decreased with increasing modulus, independent of gender ( $p = 0.17$ ), but the intercept was higher in females than males ( $p < 0.005$ , means are marked by horizontal lines on the graph).

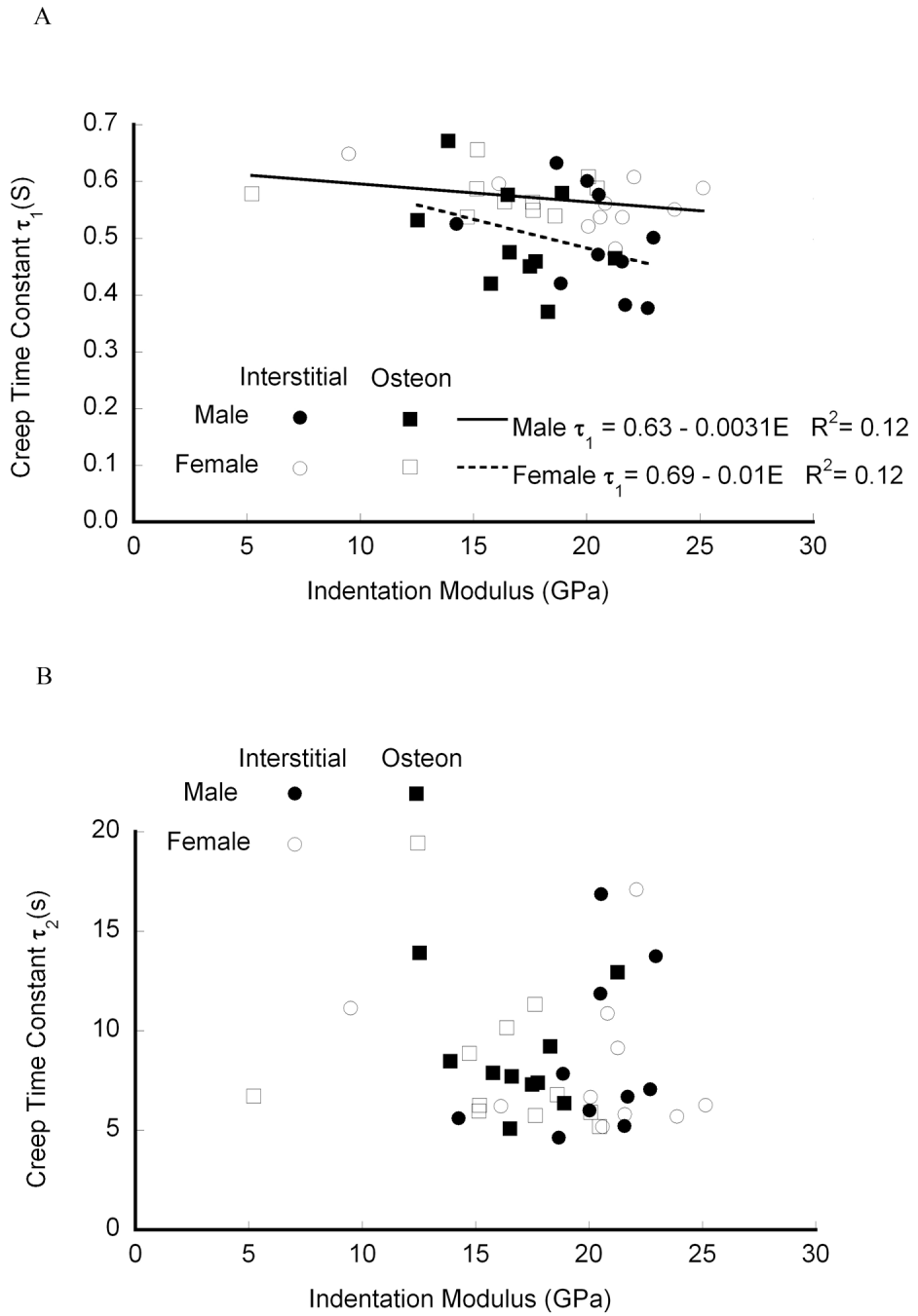


**Figure 4.** An alternate viscoelastic model, a two-dashpot Kelvin model, had differing time constants. The smaller of the two creep time constants was negatively correlated with modulus and the intercept was significantly greater for females than for males ( $p < 0.05$ ).

**Table 1**

Age and tissue composition of the sample tested (Mean  $\pm$  Standard Deviation.). None of the measured properties differed between males and females.

	Male (n = 10)	Female (n = 10)	Pooled (n = 20)
Age (yrs)	70 $\pm$ 12	76 $\pm$ 11	73 $\pm$ 11
BMD <sub>tissue</sub> (mgHA/cm <sup>3</sup> )	945.14 $\pm$ 33.29	939.72 $\pm$ 35.74	942.43 $\pm$ 33.73
Ash Density (mgHA/cm <sup>3</sup> )	921.16 $\pm$ 99.03	933.09 $\pm$ 95.38	927.12 $\pm$ 94.83
Organic Fraction (% weight)	30.04 $\pm$ 1.21	31.14 $\pm$ 1.49	30.59 $\pm$ 1.44
Collagen Content ( $\mu$ mol/mg)	0.44 $\pm$ 0.06	0.45 $\pm$ 0.05	0.44 $\pm$ 0.05
PE (mmol/mol collagen)	0.776 $\pm$ 0.746	1.263 $\pm$ 0.498	1.020 $\pm$ 0.665
HP (mol/mol collagen)	0.241 $\pm$ 0.205	0.264 $\pm$ 0.094	0.252 $\pm$ 0.156
LP (mol/mol collagen)	0.0869 $\pm$ 0.0827	0.0855 $\pm$ 0.0329	0.0841 $\pm$ 0.0640

TMD = tissue mineral density, pash = ash density, Hyp = concentration of hydroxyproline (collagen content), PE = pentosidine, HP = Hydroxylysylpyridinoline and LP = Lysylpyridinoline

**Table 2**

The Pearson's correlation matrix including nanoindentation and compositional properties. Bold entries indicate significant correlations ( $p < 0.05$ ).

	$E_{int}$	$E_{ost}$	$\tau_{int}$	$\tau_{ost}$	$\tau_{average}$	TMD	$\rho_{ash}$	Organic Fraction	Hyp	PE	HP	LP
$E_{int}$	<b>1.00</b>	<b>0.90</b>	-0.31	-0.34	<b>-0.47</b>	0.41	<b>0.50</b>	0.01	-0.11	-0.07	0.15	0.09
$E_{ost}$		<b>1.00</b>	-0.26	<b>-0.60</b>	<b>-0.48</b>	<b>0.49</b>	0.42	0.02	-0.23	-0.31	0.02	0.03
$\tau_{int}$			<b>1.00</b>	<b>0.52</b>	<b>0.91</b>	-0.30	<b>-0.59</b>	<b>0.50</b>	0.32	-0.27	-0.32	-0.34
$\tau_{ost}$				<b>1.00</b>	<b>0.83</b>	-0.09	-0.35	-0.01	-0.07	0.15	-0.11	-0.06
$\tau_{average}$					<b>1.00</b>	-0.27	<b>-0.57</b>	0.33	0.17	-0.11	-0.37	-0.27
TMD						<b>1.00</b>	0.41	-0.27	-0.42	-0.02	0.11	0.10
$\rho_{ash}$							<b>1.00</b>	-0.44	-0.17	0.22	0.37	0.31
Organic Fraction								<b>1.00</b>	<b>0.57</b>	-0.05	-0.20	-0.18
Hyp									<b>1.00</b>	0.14	-0.24	-0.36
PE										<b>1.00</b>	-0.26	0.03
HP											<b>1.00</b>	<b>0.93</b>
LP												<b>1.00</b>

$E_{int}$  = indentation modulus in interstitial tissue,  $E_{ost}$  = indentation modulus in osteonal tissue,  $\tau_{int}$  = creep time constant in interstitial tissue,  $\tau_{ost}$  = creep time constant in osteonal tissue,  $\tau_{average}$  = mean value of creep time constant in interstitial and osteonal tissue, TMD = tissue mineral density,  $\rho_{ash}$  = ash density, Hyp = concentration of hydroxyproline (collagen content), PE = pentosidine, HP = Hydroxylysylpyridinoline and LP = Lysylpyridinoline.